CellPress

Chemistry & Biology
Article

PA28αβ Reduces Size and Increases Hydrophilicity of 20S Immunoproteasome Peptide Products

Mary Raule,[1] Fulvia Cerruti,[1] Nadia Benaroudj,[2] Rebekka Migotti,[3] Julia Kikuchi,[3] Angela Bachi,[4] Ami Navon,[5] Gunnar Dittmar,[3] and Paolo Cascio[1,*]

[1]Department of Veterinary Sciences, University of Turin, 10095 Grugliasco, Italy
[2]Unité Biologie des Spirochètes, Institut Pasteur, 75015 Paris, France
[3]Mass Spectrometry Core Unit, Max-Delbrück Center for Molecular Medicine, 13125 Berlin, Germany
[4]IFOM, FIRC Institute of Molecular Oncology, 20139 Milan, Italy
[5]Department of Biological Regulation, The Weizmann Institute of Science, 76100 Rehovot, Israel
*Correspondence: paolo.cascio@unito.it
http://dx.doi.org/10.1016/j.chembiol.2014.02.006

SUMMARY

The specific roles that immunoproteasome variants play in MHC class I antigen presentation are unknown at present. To investigate the biochemical properties of different immunoproteasome forms and unveil the molecular mechanisms of PA28 activity, we performed in vitro degradation of full-length proteins by 20S, 26S, and PA28αβ-20S immunoproteasomes and analyzed the spectrum of peptides released. Notably, PA28αβ-20S immunoproteasomes hydrolyze proteins at the same low rates as 20S alone, which is in line with PA28, neither stimulating nor preventing entry of unfolded polypeptides into the core particle. Most importantly, binding of PA28αβ to 20S greatly reduces the size of proteasomal products and favors the release of specific, more hydrophilic, longer peptides. Hence, PA28αβ may either allosterically modify proteasome active sites or act as a selective "smart" sieve that controls the efflux of products from the 20S proteolytic chamber.

INTRODUCTION

The continual presentation of intracellular protein fragments on major histocompatibility complex (MHC) class I molecules is a process that allows cytotoxic $CD8^+$ T lymphocytes (CTLs) to eliminate cells that synthesize foreign or abnormal proteins (Pamer and Cresswell, 1998). The vast majority of MHC class I-presented peptides are generated during the degradation of mature proteins or defective ribosomal products by the ubiquitin-proteasome system (UPS) (Rock and Goldberg, 1999; Yewdell, 2001). The active form of proteasome, which appears to degrade most cellular proteins, is the 26S proteasome, a large proteolytic complex formed by the association of the 19S regulatory particle with the 20S proteasome (Voges et al., 1999). In most cells, the proteolytic activity of the 20S proteasome is mediated by three subunits of the core particle: β5, β2, and β1. However, lymphoid cells and cells exposed to cytokines such as interferon γ (IFN-γ) express three alternative, homologous subunits (β5i/LMP7, β2i/MECL-1, β1i/LMP2), which replace the constitutive active β-subunits in newly-assembled immunoproteasome particles (Kloetzel, 2001). The pivotal role of immunoproteasomes in the generation of MHC class I ligands was recently demonstrated in transgenic mice lacking all three proteasomal catalytic β-immune subunits (Kincaid et al., 2012).

Another IFN-γ-inducible UPS component that affects MHC class I antigen presentation is PA28, a ring-shaped heteroheptameric complex (3α4β) (Sugiyama et al., 2013) that can bind to the 20S proteasome and dramatically enhance its ability to degrade short peptide substrates, but not ubiquitin-conjugated proteins (Dubiel et al., 1992; Ma et al., 1992). In addition, PA28 can also form an asymmetric 26S hybrid complex (19S-20S-PA28) (Cascio et al., 2002; Hendil et al., 1998). The effects of PA28 on antigen processing and $CD8^+$ responses are still unclear and controversial (Rechsteiner et al., 2000). Expression of PA28α or PA28αβ has been reported to enhance MHC class I presentation of some, but not all, antigens (Sijts et al., 2002). Furthermore, cells lacking this complex have a reduced ability to generate certain antigens (Murata et al., 2001). Recent studies have identified PA28 as the second most important UPS component for the production of MHC class I ligands (de Graaf et al., 2011), although its effects seem to be restricted to specific MHC class I alleles (Yamano et al., 2008). Additionally, several studies have indicated that oxidized proteins are preferentially degraded without ubiquitination by 20S immunoproteasomes (Orlowski and Wilk, 2003) in a process that may be stimulated by PA28αβ (Li et al., 2011; Pickering et al., 2010). A variety of biochemical actions have been proposed for PA28 (Rechsteiner et al., 2000; Stadtmueller and Hill, 2011), and the crystal structure of PA26 (PA28 homolog in trypanosomes) in association with 20S yeast proteasomes has been solved (Whitby et al., 2000). The binding of PA26 was found to dilate the gated channel in the proteasome α-ring through which substrates enter (Groll et al., 2000) and products exit (Köhler et al., 2001). Therefore, PA28 was predicted to lead to attenuation of proteasomal processivity and consequent release of peptide products with a greater mean length (Whitby et al., 2000), as occurs upon deletion of the α-gate (Köhler et al., 2001). A full understanding of the molecular mechanism of PA28 activity would undoubtedly represent an important achievement, especially in light of the observation that mammalian cells contain significant amounts of PA28αβ-20S immunocomplexes (Ahn et al., 1996; Hendil et al., 1998), whose abundance further increases upon IFN-γ stimulation (Murata et al., 2001; Tanahashi et al., 1997).

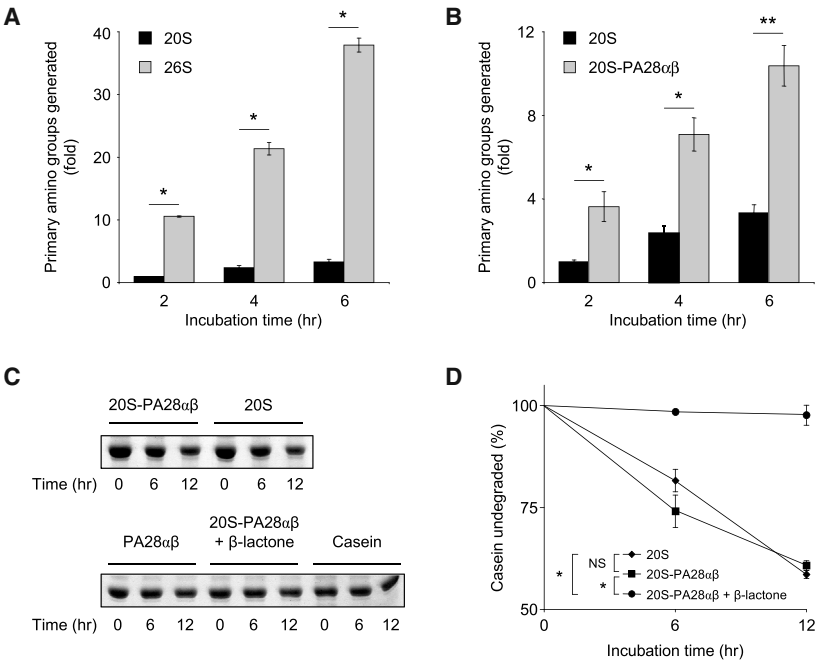

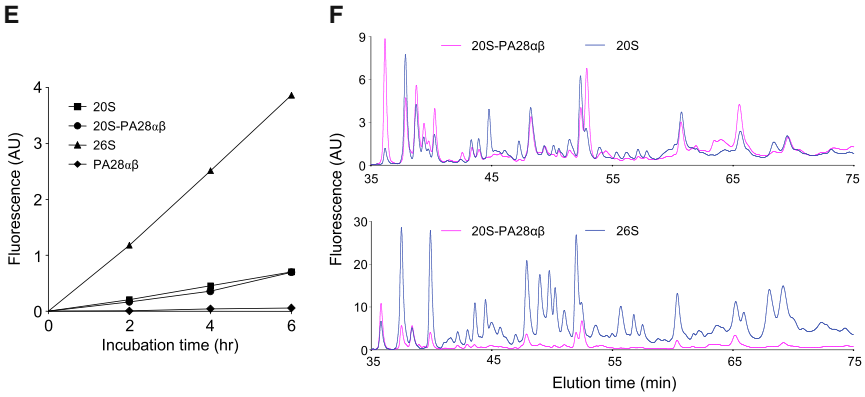

Figure 1. Casein Degradation by 20S, 26S, and PA28αβ-20S Immunoproteasomes

(A and B) Primary NH2 generated by equimolar amounts of immunoproteasomes were quantified by fluorescamine and are expressed as fold change relative to the amount released in 2 hr by 20S. (A) Equimolar amounts of 20S and 26S. (B) Equimolar amounts of 20S and PA28αβ-20S. The average of four to six independent experiments (±SEM) is shown. NH2 generation does not occur when the substrate was incubated alone, with only PA28αβ or in the presence of β-lactone. *$p < 0.05$, **$p < 0.01$. See also Figure S1.

(C) Casein was incubated as indicated in the figure, and the undegraded protein was separated by SDS-PAGE.

(D) Densitometric quantification of the residual protein. Data are the average of three independent experiments (±SEM). NS, not significant. *$p < 0.05$.

(E) FITC-casein was incubated with immunoproteasomes, and generation of soluble fluorescence was assessed. AU, arbitrary units.

(F) FITC-casein was degraded by immunoproteasomes, and peptides were analyzed by RP-HPLC. See also Experimental Procedures.

RESULTS

Different Immunoproteasome Species Exhibit Distinct Rates of Peptide Bond Cleavage and Turnover of Protein Substrates

In an attempt to further characterize the biochemical properties of different forms of IFN-γ-induced proteasomes, we incubated casein for several hours with 26S, 20S, and 20S-PA28αβ immunoproteasomes in a buffer containing ATP and Mg^{2+}, and the hydrolysis of the substrate was measured by fluorescamine assay (Cascio et al., 2001; Kisselev et al., 1999). Under these experimental conditions, proteasome species are completely stable and maintain their structural integrity and biochemical properties for several hours (Cascio et al., 2001; Kisselev et al., 1999) (Figure S1A available online). As shown in Figures 1A and 1B, the rates of generation of new amino groups were linear, albeit widely different, for up to 6 hr for the three immunoproteasome species analyzed. Specifically, 26S immunoproteasomes were found to generate ~10-fold more amino groups than 20S immunoproteasomes (Figure 1A). Surprisingly, the 20S-PA28αβ complexes consistently generated 3-fold more amino groups at each time point than 20S particles alone (Figure 1B). This observation was unexpected because PA28 has been described as an activator of hydrolysis by the 20S particle of small tri- and tetrapeptides (but not full-length proteins) (Ma et al., 1992). In principle, the higher generation rate of primary amino groups by PA28αβ–associated 20S immunoproteasomes might result from either accelerated protein breakdown induced by the activator or from a modification in the pattern of peptide products released (i.e., even if the overall rate of substrate consumption were not increased). To discriminate between these two mechanisms, we initially followed the disappearance of undigested casein incubated for several hours in the presence of 20S immunoproteasomes alone or conjugated with PA28. This experiment clearly demonstrated that the presence of PA28αβ does not modify the kinetics of substrate disappearance (Figures 1C and 1D). The lack of increased substrate consumption upon binding of PA28αβ to the 20S core particle was subsequently confirmed by assessing degradation of fluorescein isothiocyanate (FITC)-labeled casein (Figure 1E). In this assay, the fluorescence signal generated is directly proportional to the rate of turnover of the substrate independently of the characteristics of the peptides produced. As shown in Figure 1E, the rates of appearance of trichloroacetic acid-soluble fluorescence were identical when FITC-casein was degraded by either 20S or 20S-PA28αβ particles and were nearly 6-fold lower than rates observed with 26S immunoproteasomes. We therefore concluded that the association of PA28 with 20S immunoproteasomes does not alter the rate of casein and FITC-casein hydrolysis. Accordingly, we tested whether PA28αβ might

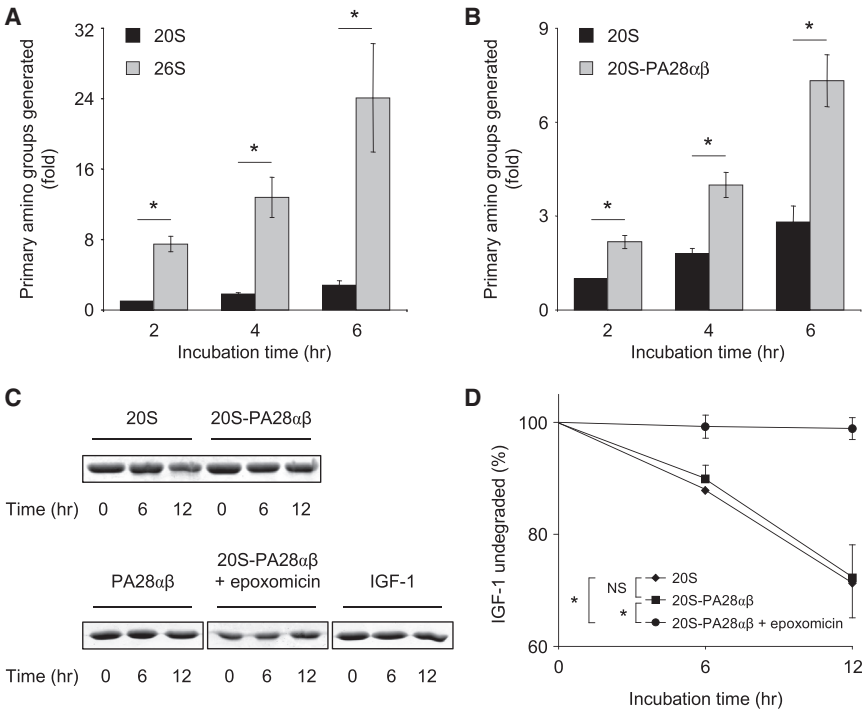

Figure 2. IGF-1 Degradation by 20S, 26S, and PA28αβ-20S Immunoproteasomes

(A and B) Degradation of IGF-1 immunoproteasomes was performed as described in Figure 1. (A) Degradation by 20S and 26S. (B) Degradation by 20S and PA28αβ-20S. The average of three independent experiments (±SEM) is shown. *$p < 0.05$.

(C) IGF-1 was incubated as indicated, and the undegraded protein was separated by SDS-PAGE.

(D) Densitometric quantification of the residual protein. Data are the average of three independent experiments (±SEM). NS, not significant. *$p < 0.05$.

modify the pattern of peptides generated from these substrates, presumably by increasing the frequency of cleavage within the 20S core. Toward this end, we separated degradation products by reverse phase high-performance liquid chromatography (RP-HPLC), and the chromatographic profiles were compared. Remarkably, the peptide patterns were dramatically different depending on whether FITC-casein (Figure 1F) was degraded by the 20S, 20S bound to PA28, or 26S immunoproteasomes. In particular, although some peptides were produced by both 20S and 20S-PA28 particles, albeit in different amounts, several others were detected only when one of these two immunoproteasome forms was used (Figure 1F).

To confirm these findings, we performed similar degradation experiments with the 8 kDa protein insulin-like growth factor 1 (IGF-1), another well-characterized proteasome model substrate. Similar to what has been observed for casein, the rates of appearance of primary amino groups were ~8-fold and ~2-fold higher than 20S particles for 26S and for 20S-PA28αβ immunoproteasomes, respectively (Figures 2A and 2B). Importantly, even for IGF-1, enhanced levels of peptide bond cleavage induced by PA28 did not correspond to increased rates of substrate turnover, but they did to a higher frequency of cleavage events (Figures 2C and 2D).

20S-PA28αβ Complexes Generate Shorter Peptide Products than 20S and 26S Immunoproteasomes

Because the association of PA28αβ with 20S particles did not alter the rate of protein hydrolysis but did modify the pattern of the peptides produced, we investigated the effect of this association on the size distribution of proteasomal products. In fact, because the observed increase in the rate of peptide bond cleavage does not result in enhanced substrate turnover, it must be correlated with a reduction in the average size of peptide products. To test this hypothesis, we incubated casein and IGF-1 with the 20S, 20S-PA28αβ, and 26S immunoproteasomes under conditions that ensure a linear rate of peptide generation and do not favor a second cycle of cleavage following release from proteasomes (Cascio et al., 2001; Kisselev et al., 1999). To ensure such conditions, substrates were present in large excess and no more than 10% of the initial substrate was consumed (Figures S2A and S2B). After 6 hr, the peptides produced were separated from the undigested substrate by ultrafiltration through a 5 kDa membrane, derivatized with fluorescamine, and fractionated by high-performance size exclusion chromatography (HP-SEC) with online fluorescence detection. This method provides a quantitative measure of different products, as the intensity of the fluorescence signal emitted by any peptide is the same and is independent of its length (Berko et al., 2012; Köhler et al., 2001). When analyzed by this method, peptides generated from casein by the 20S and 26S immunoproteasomes were found to fall into a continuum of size distribution ranging from 1 to 26 residues (Figure 3A) that appeared to fit a lognormal distribution, which is in agreement with previous analyses of different substrates and proteasome species (Cascio et al., 2001, 2002; Kisselev et al., 1999; Köhler et al., 2001). Specifically, the chromatographic profile of 20S particle products was characterized by four broad peaks (Figure 3A, left panel) corresponding to lengths of 1 or 2, 3–5, 11–13, and 17–20 residues. The generation of detectable amounts of products with a molecular weight of ~200 Da was unexpected because proteasomes have not been found to generate such small fragments. It is possible that the analytical approaches used previously either excluded or imposed a strong bias against individual amino acids and dipeptides, whereas the method we used in this study can accurately separate and quantitate peptides between 1 and 30 residues long (Figure S2C). A similar size distribution was also obtained for the products of 26S immunoproteasomes, although in this case the peak of the longer fragments was significantly reduced and a matching increase was detected in the peaks corresponding to the shorter peptides (Figure 3A, right panel). Consequently, both the mean and median lengths of peptide products were about two residues shorter for 26S than for 20S

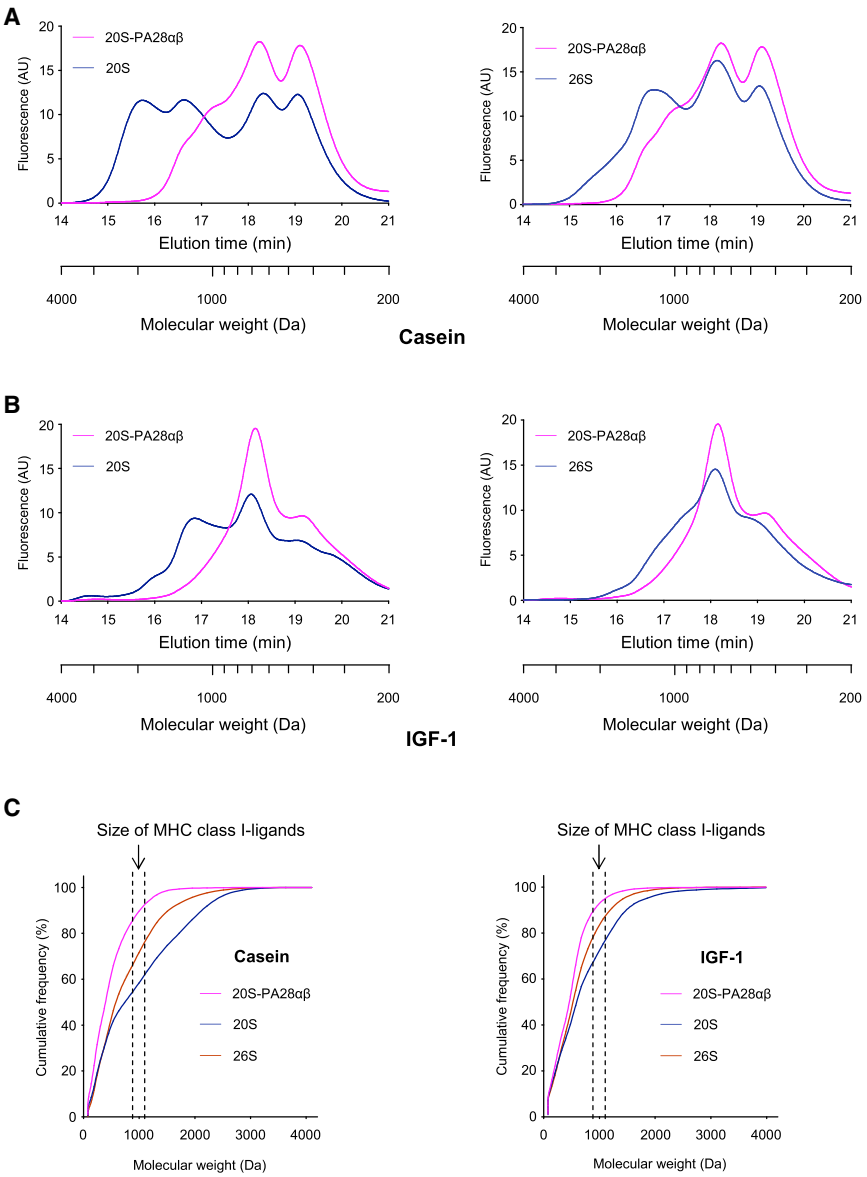

Figure 3. Size Distribution of Peptides Generated from Casein and IGF-1 by 20S, 26S, and PA28αβ-20S Immunoproteasomes

(A and B) Equal amounts of peptides generated during degradation by 20S, 26S, and PA28αβ-20S immunoproteasomes were reacted with fluorescamine and immediately fractionated by HP-SEC. (A) Degradation of casein. (B) Degradation of IGF-1. Similar data were obtained in at least four independent experiments.

(C) The cumulative frequency curves of peptides generated from casein and IGF-1 were obtained by transformation of data shown in (A) and (B). For each molecular weight, the fraction of peptides with this molecular mass and lower was calculated, and each curve was obtained by averaging the data from four independent experiments. See also Figure S2 and Experimental Procedures.

immunoproteasomes (Table 1). However, the size distribution of products generated by 20S-PA28αβ immunoproteasomes differed drastically from that of both 20S and 26S particles (Figure 3A). Specifically, the peak corresponding to the longer products disappeared, the peak of 11- to 13-residue peptides was significantly reduced, and the two peaks of shorter fragments increased in size. Consequently, the binding of PA28αβ to 20S proteasomes reduced the mean and median sizes of peptide products by about 50% (Table 1).

Similar results were subsequently obtained for the size distributions of IGF-1 degradation products (Figure 3B). With this shorter substrate, 20S immunoproteasomes were found to generate the same four broad peaks of products we had already observed for casein, although in this case the two central peaks were higher than the peaks of longer and smaller fragments (Figure 3B, left panel). Furthermore, with 26S particles, the peak of 11–13 amino acids was also strongly reduced (Figure 3B, right panel), whereas with 20S-PA28αβ immunoproteasomes, a major peak (corresponding to three to five residues) was detected and the peak of amino acids and dipeptides slightly increased in size compared to 20S and 26S (Figure 3B). Accordingly, the mean and median product lengths calculated from these size distributions were higher for 20S than for 26S immunoproteasomes, whereas 20S-PA28αβ products were characterized by lower mean and median values (Table 1).

To further analyze the relative distributions of peptides of different sizes, we plotted these data as cumulative frequency curves (Kisselev et al., 1999) (Figure 3C). The resulting size distribution plots clearly showed that, for both protein substrates, no more than 10% of peptides generated by the three forms of immunoproteasomes were eight to ten residues long, which is the appropriate length to bind MHC class I heterodimers (Figure 3C and Table 2). Importantly, the association of PA28αβ with the 20S particles did not increase this fraction, but slightly reduced it (Table 2). Moreover, casein products that might serve in MHC class I antigen presentation after appropriate trimming by aminopeptidases in the cytosol or the endoplasmic reticulum (ER) represent 38%, 24%, and 8% of the total when the protein is degraded by 20S, 26S, and 20S-PA28αβ immunoproteasomes, respectively (Figure 3C and Table 2). Similar results were obtained for IGF-1, although with this smaller substrate higher production of peptides shorter than eight residues were detected for all three immunoproteasome species (Figure 3C and Table 2).

Tandem Mass Spectrometry of Immunoproteasomal Products

To further define changes in the patterns of products that resulted from binding of PA28αβ to 20S particles, and specifically

Table 1. Mean Peptide Sizes Generated by 20S, 20S-PA28αβ, and 26S Immunoproteasomes from IGF-1 and Casein

Immunoproteasome	Substrate	Mean	Median
20S	IGF-1	7.3 ± 0.10	5.9 ± 0.07
	casein	9.4 ± 0.14	7.3 ± 0.27
20S-PA28αβ	IGF-1	4.9 ± 0.07	4.6 ± 0.04
	casein	4.8 ± 0.05	3.9 ± 0.07
26S	IGF-1	6.0 ± 0.05	5.3 ± 0.06
	casein	7.3 ± 0.04	5.7 ± 0.10

Mean sizes and medians were calculated using the product distributions obtained by HP-SEC, assuming an average molecular weight of 110 Da for each residue. Values are averages from five experiments (±SEM).

Table 2. Size Classes of Peptides Generated from IGF-1 and Casein by Different Forms of Immunoproteasomes

		Fractions of Peptides (%)		
Immunoproteasome	Substrate	<8 aa	8–10 aa	>10 aa
20S	IGF-1	67	9	24
	casein	54	8	38
20S-PA28αβ	IGF-1	89	6	5
	casein	86	6	8
26S	IGF-1	78	9	13
	casein	66	10	24

Peptide lengths were calculated using the product distributions obtained by HP-SEC and grouped into three size classes to fit into the groove of MHC class I molecules: longer (>10 aa), shorter (<8 aa), and of the correct size (8–10 aa).

to investigate in detail the nature of the differences observed between 20S, 20S-PA28αβ, and 26S immunoproteasomes, the individual peptides generated from IGF-1 and casein were analyzed by tandem mass spectrometry (MS/MS). In the MS/MS analysis, we excluded peptides with a length of up to seven amino acids in order to minimize signals originating from small chemical compounds. Although MS/MS does not provide quantitative information about the absolute abundance of the peptides detected, their relative amounts can be assessed by comparing the corresponding ion intensities measured in sequential MS/MS analyses (Bantscheff et al., 2007; Old et al., 2005). Therefore, we used ion intensities to quantify the relative amount of single fragments generated from IGF-1 and casein by more than one immunoproteasome species. By using this approach, 90 different peptides from IGF-1 and 103 from casein were unambiguously identified and quantified (Figure 4). These peptides ranged in length from 8 to 25 residues and were derived from the entire length of the proteins. Notably, the generation of some of the peptides required the removal of one or two residues from the substrate, further demonstrating that proteasomes can release products as short as single amino acids and dipeptides. Most importantly, this analysis demonstrated that, though some peptides are generated exclusively by the 20S, 20S-PA28αβ, and/or 26S immunoproteasomes, several others are produced in common by different immunoproteasome forms, but in very different amounts. In fact, even if some products are released at about the same level by two or even all three proteasome species, many others are characterized by striking quantitative differences spanning over three log values. Notably, regardless of the clear differences in the overall sizes distributions of products unveiled by HP-SEC, the MS/MS data reveal that each of the three immunoproteasome forms can preferentially enhance the generation of individual peptides that are 8–25 residues in length (Figure 4 and Table S1). These results were further confirmed by the analysis of peptides generated by the asymmetric 26S hybrid complex: namely, proteasomes capped at one side by 19S regulatory particles and by PA28 at the other (Cascio et al., 2002; Hendil et al., 1998). In this case, MS/MS analysis revealed that hybrid particles generate some of the peptides produced in common by 26S and PA28αβ-20S from IGF-1 and also several of those released specifically only by one of the two immunoproteasome forms (Table S2).

To check whether the differences in the sequence of products revealed by MS/MS analysis might be predicted at least in part on the basis of the modifications of the three main proteasomal peptidase activities induced by PA28, we assessed the stimulatory effect of PA28 on cleavage specificities of 20S particles. In this way, we found that the caspase-like activity, although lower in absolute terms, is the immunoproteasome peptidase activity that is enhanced to a higher extent by PA28, whereas stimulation of chymotryptic and tryptic activities appears to be lower and more dependent on the specific sequence of the peptide used (Figure 5A). It is interesting that this higher activation of caspase-like activity may help to explain the enhanced generation of peptides with an acidic residue at their C terminus that we observed when IGF-1 and, to a lesser extent, casein are degraded by 20S-PA28αβ particles (Figure 4 and Table S1). Furthermore, in an attempt to define the physiochemical parameters that control the generation of longer products in the presence of PA28, we calculated the hydropathy of peptides exclusively (or preferentially) released by 20S and PA28αβ-20S immunoproteasomes (Table S3). As expected for products derived from two extremely hydrophilic proteins, such as IGF-1 and casein, both pools of peptides were characterized by high average hydrophilicity. However, hydrophilicity was significantly higher for peptides generated by PA28αβ-20S immunoproteasomes (Figure 5B), suggesting that PA28 might allow preferential release of longer products that are polar and/or charged from the proteolytic proteasomal chamber.

DISCUSSION

In the present study, we focused on immunoproteasomal degradation of loosely folded, nonubiquitinated proteins, as ubiquitinated proteins are not hydrolyzed by 20S and PA28-20S complexes (Dubiel et al., 1992; Ma et al., 1992), most likely because these particles lack the enzymatic activities necessary to remove and/or to unfold polyubiquitin chains that otherwise would sterically block translocation of substrates into the proteolytic chamber (Shabek and Ciechanover, 2010; Yao and Cohen, 2002). As a result, we found that unstructured polypeptides are hydrolyzed at rates that are nearly 10-fold higher by 26S compared to 20S immunoproteasomes. This finding is consistent with the notion that the free 20S particle is a relatively inactive protease, presumably because the N-terminal tails of its α subunits obstruct the two opposite axial pores through which

substrates access the internal catalytic lumen (Groll et al., 2000). This autoinhibited state is relieved when the 20S core particle binds to activators, such as 19S or PA28, that displace the N-terminal tails, thereby opening an axial channel in the α-ring (Köhler et al., 2001; Whitby et al., 2000). However, the latency of unliganded 20S proteasome is not absolute, because, even in the absence of artificial treatments that are known to activate it (Coux et al., 1996), the 20S core particle degrades proteins at detectable and reproducible rates, probably involving transient and/or only partial channel opening (Köhler et al., 2001). Accordingly, atomic force microscopy studies have shown that the α-rings of the 20S proteasome repeatedly switch between an open and a closed gate conformation, and, importantly, the relative abundance of the two conformers depends on the nature of their interaction with ligands. In fact, the closed conformation predominates in control or inhibited 20S proteasomes, whereas the open form prevails in the presence of peptide or protein substrates (Osmulski and Gaczynska, 2000, 2002; Osmulski et al., 2009). Interestingly, despite the fact that the open-channel conformation of the gating residues induced by ATP-dependent (i.e., 19S) and ATP-independent (i.e., PA28) activators appears to be identical (Rabl et al., 2008), our data show that PA28αβ-20S immunocomplexes hydrolyze proteins at the same rates as 20S immunoproteasomes and much less efficiently than 26S immunoproteasomes. These results confirm the initial reports on the biochemical properties of PA28 (Ma et al., 1992), but it appears to be difficult to reconcile them with the known role of the proteasomal gate in controlling accessibility of substrates into the lumen of the 20S particle. In fact, opening of the axial channel by deletion of the N-terminal tails of eukaryotic (Köhler et al., 2001) or archaeal (Benaroudj et al., 2003) proteasomal α subunits results in strong enhancement of the degradation rates of unfolded proteins, suggesting that unstructured substrates can freely access the internal proteolytic chamber of the 20S particle simply by passive diffusion thorough a fully open gate. In light of these data, the inability of PA28 to enhance hydrolysis rates of loosely folded proteins is surprising. In fact, the crystal structure of PA28α shows that the aqueous channel through the heptamer has a diameter of 20 Å at its minimum, which is at least in principle wide enough for passage of unfolded proteins (Knowlton et al., 1997). However, the homolog-specific inserts present between helices 1 and 2, which are not resolved in the crystal structure, most likely form a ringlike collar on the upper, non-proteasome binding surface of the PA28 heptamer. Although several studies have shown that these loops do not restrict passage of tri- or tetrapeptide fluorogenic substrates (Song et al., 1997; Zhang et al., 1998), recent investigations have demonstrated that they can hinder the transit of longer peptides, and conceivably of proteins as well, through the PA28 channel (Sugiyama et al., 2013).

Although PA28αβ does not enhance the rates of protein degradation by proteasomes, its association with the 20S particle leads to profound changes in the patterns of the generated peptides, which greatly differ from those produced by 20S and 26S immunoproteasomes. In fact, from both protein substrates analyzed, 20S and 26S immunoproteasomes were found to release a continuum of peptides with a size ranging from 1 to 26 residues, although some classes of length clearly predominate. Surprisingly, PA28αβ-20S immunoproteasomes display a reduced ability to generate longer products that, in principle, might depend upon different mechanisms. Conceivably, PA28 might stimulate additional rounds of hydrolysis of previously digested, longer precursors. However, reentry into the proteasome and further hydrolysis of already released fragments seem statistically less likely because our degradation assays were performed under conditions that have previously been shown to allow generation of individual peptides at linear rates for several hours (Cascio et al., 2001; Kisselev et al., 1999). To this end, substrate was always present in large excess, and no more than 10% of the protein was consumed at the end of the incubation period, which ensured that peptides analyzed were generated directly from the substrate and did not reenter the proteasome and undergo cleavage in later rounds of proteolysis. Likewise, it has been shown that in vitro peptides released by proteasomes are further cleaved by these proteolytic particles at extremely low rates (Saric et al., 2004), and they are therefore unlikely to efficiently compete for degradation with proteins, which are much more preferable as substrates (Dolenc et al., 1998). Furthermore, if reuptake and further hydrolysis by 20S-PA28αβ immunoproteasomes of intermediate fragments had occurred, they would have been expected to increase over time as longer peptides were generated and their concentration increased. Consequently, the kinetics of new amino group generation would most likely be exponential rather than linear because intermediate fragments would be metabolized again according to a double-cut modality, which implies release of three free amino groups each time a long precursor is further hydrolyzed (Dick et al., 1996). If intermediate products were indeed generated, over time they would start to compete with the protein substrates for hydrolysis at proteasomal active sites, which in turn would cause a progressive decrease in the rates of protein consumption, a phenomenon that we did not observed even after prolonged incubation. As alternative possibilities, PA28 might enhance generation of shorter products by inducing conformational changes in proteasomal active sites or by imposing a constraint on the exit port that would have a greater effect on longer fragments. These fragments would be retained inside the proteasomal proteolytic cavity longer and therefore would have an increased probability of further cleavage. At the present, neither of these two hypotheses can be controverted. In fact, although crystallographic studies show that association with PA26 does not induce structural modification of proteasomal catalytic β subunits (Whitby et al., 2000), biochemical data indicate that proteasomal proteolytic sites are allosterically regulated (Harris et al., 2001; Li et al., 2000, 2001) and that their modification leads to gate opening (Osmulski and Gaczynska, 2000, 2002; Osmulski et al., 2009). Furthermore, an allosteric pathway linking the PA26 binding sites with the active sites in the *Thermoplasma acidophilum* 20S proteasome has recently been described (Ruschak and Kay, 2012). A model entailing PA28αβ in which it acts by imposing a constraint on diffusion of longer products out of the hydrolytic chamber, thus facilitating their further hydrolysis, is also consistent with our data. In this scenario, PA28 would primarily act as a sieve that retains longer protein fragments inside the 20S proteolytic chamber until they were cleaved to pieces small enough to diffuse outside the chamber. Such a molecular mechanism would be consistent with both detailed kinetic analysis showing that PA28 exerts its activating

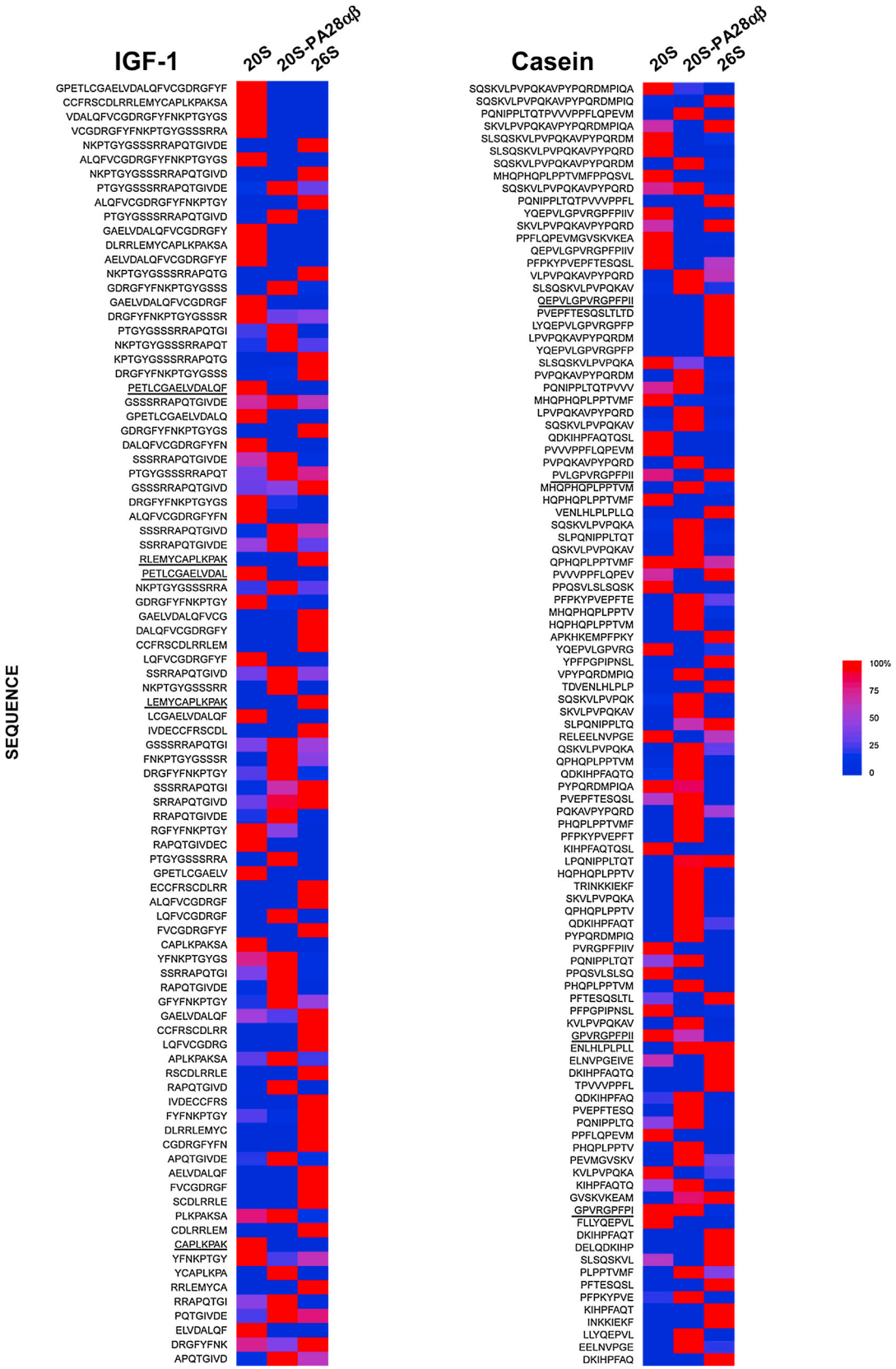

(legend on next page)

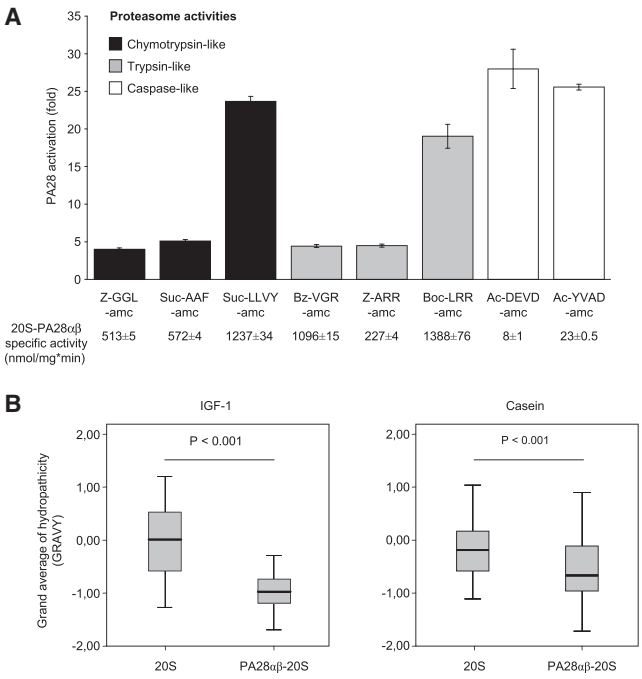

Figure 5. Modifications in Cleavage Specificities of 20S Immunoproteasomes Induced by PA28αβ

(A) Chymotryptic, tryptic, and caspase activities of the PA28αβ-20S immunoproteasome were measured with different fluorogenic peptides and are indicated as fold change relative to the corresponding activities of the 20S particle alone. Data are the average of three independent experiments (±SEM). Below the graph, the values (±SEM) of specific activity for the hydrolysis of each fluorogenic substrate by PA28αβ-20S are reported. See also Supplemental Information.

(B) The grand average of hydropathy values for peptides preferentially released from IGF-1 and casein by 20S and PA28αβ-20S immunoproteasomes were calculated as described in Table S3.

influence by enhancing bidirectional passage of short peptides (three or four residues) (Stohwasser et al., 2000) and with a previous in vitro/in silico study that identified one of the major factors involved in the enhancement of double-cut efficiency induced by PA28 in a reduced efflux of longer peptides out of the 20S particle (Mishto et al., 2008). Furthermore, it was recently shown that a PA28αβ complex lacking the unstructured and highly mobile PA28α loops surrounding the central pore of the heptameric ring cleaves substrates longer than a nonapeptide more efficiently than wild-type PA28. On these bases, it was hypothesized that the flexible loops of PA28 might act as gatekeepers that block the exit of longer peptides from the proteolytic chamber (Sugiyama et al., 2013). Selectivity based exclusively on peptide size, however, cannot account for the global effects of PA28 on the patterns of proteasome products observed in our study. In fact, quantitation of products demonstrated that several individual peptides with a length of 8 to 23 residues are released in much higher amounts by PA28αβ-20S than by 20S or 26S immunoproteasomes (Table S1). At present, the properties that might allow specific longer peptides to evade the constraint imposed by PA28 toward their efflux are not completely clear. However, the finding that products longer than seven residues whose generation is strongly enhanced in the presence of PA28 are, on average, more hydrophilic than those preferentially released by 20S alone, suggesting that the passage of polar and/or charged long peptides thorough PA28 might be favored. In this model, PA28 would act as a selective "smart" sieve that strictly controls the exit from proteasomes of products on the basis of size and, presumably, sequence. As a result, PA28αβ would promote preferential efflux from the 20S proteolytic cavity of only a reduced number of individual peptides longer than six or seven amino acids, whereas the great majority of the other proteasomal products would be retained inside, where they would further cleave to smaller pieces before they diffused outside. In accordance with this model, the central channel of the PA28α ring is almost completely lined by charged or polar residues (Knowlton et al., 1997) and is thus well-suited for permitting the passage of water-soluble peptides. Importantly, this molecular model would also be consistent with our findings regarding 19S-20S-PA28 immunoproteasomes. In this case, the absence of a clear difference in size distribution (Cascio et al., 2002) supports the hypothesis that, in hybrid proteasomes (as in 26S canonical particles), the main route of exit of peptides from the inner proteolytic chamber is regulated by the 19S cap, whereas PA28 exerts its major effect by allowing preferential sorting, through its central channel, of selected products. Accordingly, hybrid particles were found to generate some of the peptides produced in common by 26S and PA28αβ-20S from IGF-1, in addition to several of those released specifically by only one of the two immunoproteasome forms.

Implications for MHC Class I Antigen Presentation

The reasons why mammalian cells are equipped with different immunoproteasome species and whether these immunoproteasomal variants play specific roles in the MHC class I antigen-processing pathway are presently unknown. Yet, the in vivo observation that their cellular levels greatly increase following IFN-γ stimulation (Murata et al., 2001; Tanahashi et al., 1997) strongly supports their involvement in MHC class I presentation. In this regard, the major findings of our study can be summarized as follows.

(1) For both protein substrates analyzed, only ~10% of peptides generated by 20S and 26S immunoproteasomes are eight to ten residues long, which is the appropriate length to bind MHC class I heterodimers. Most importantly, association of PA28αβ with the ends of 20S immunoproteasomes does not increase the fraction of the eight- to ten-residue peptides generated, but reduces it to 6% of the total for both substrates.

(2) The fraction of peptides longer than ten amino acids, which might serve in MHC class I antigen presentation

Figure 4. MS/MS Analysis of Peptides Generated from IGF-1 and Casein Degradation by 20S, 26S, and PA28αβ-20S Immunoproteasomes

Peptides were identified by MS/MS, and those produced by more than one immunoproteasome species were quantified on the basis of their ion intensity signal as described in the Experimental Procedures section. Values are the percentage of the highest ion intensity signal for each single peptide set as 100%. Underscored peptides are those whose generation requires removal of only one or two residues at the N or C terminus of the substrate. See also Tables S1 and S2.

only after appropriate trimming by aminopeptidases in the cytosol or ER, is larger for 20S than for 26S immunoproteasomes. Binding of PA28αβ to the 20S particle dramatically reduces the overall efficiency of generation of these longer products. We conclude, therefore, that PA28 does not act simply by expending the fraction of proteasomal products that can be accommodated in the groove of MHC class I molecules directly or after trimming.

From an immunological point of view, however, the sequence and not only the length of proteasomal products is a crucial parameter. In the present study, the relative amounts of individual peptides produced by more than one immunoproteasomal species from IGF-1 and casein were quantified on the basis of their ion intensity signal following sequencing using MS/MS. This analysis revealed striking quantitative differences, which in several cases exceeded three orders of magnitude, thus demonstrating that each immunoproteasomal form possesses the capacity to preferentially release individual peptides in the range of 8 to 25 residues. The outcome of this selection process upon MHC class I presentation is further amplified by the fact that, overall, the absolute generation of longer peptides was reduced upon association with PA28, as shown by HP-SEC analysis.

SIGNIFICANCE

Our study demonstrates that, in spite of their different general efficiency in generating products with a size distribution appropriate to serve in MHC class I presentation, 20S, 26S, and PA28αβ-20S immunoproteasomes possess the capacity to produce exclusively, or at least in a preferential manner, a subset of specific peptides. In this regard, the finding that PA28αβ induces generation of a certain number of peptides with an acidic C terminus is counterintuitive because these products cannot bind efficiently to MHC class I molecules (Kloetzel, 2001; Pamer and Cresswell, 1998; Rock and Goldberg, 1999). However, several of the remaining peptides do present the correct hydrophobic or basic C-terminal anchor residue required for association with the MHC class I groove. It seems plausible, therefore, that a substantial fraction of peptides specifically released by PA28αβ-20S immunoproteasomes might be critical in eliciting an effective CTL response under different pathophysiological conditions, especially if favoring a noncanonical, ubiquitin-independent proteolytic pathway (Orlowski and Wilk, 2003; Qian et al., 2006; Yuksek et al., 2009). In principle, it is also possible that, by promoting release of a certain number of peptides that cannot serve in MHC class I antigen presentation, PA28 might exert a regulatory function blunting excessive cytotoxic responses against antigens of self-origin, thus preventing the risk of potentially harmful autoimmune reactions.

EXPERIMENTAL PROCEDURES

Protein Purification, Substrate Degradation, and Peptide Analysis

Purification of immunoproteasomes and PA28αβ, casein and IGF-1 degradation, and HPLC analysis of peptide products were performed as previously described (Berko et al., 2012; Cascio et al., 2001, 2002; Song et al., 1997). More details are provided in the Supplemental Information. Heterodimeric PA28 (Figure S1C) was reconstituted from purified recombinant α and β subunits as described previously (Song et al., 1997), with minor modifications. Briefly, equal volumes of proteins at a final concentration of 0.1 mg/ml were preincubated in 20 mM 2-[4-(2-hydroxyethyl)piperazin-1-yl]ethanesulfonic acid (HEPES), pH 7.6, 20 mM NaCl, 1 mM EDTA, 5 mM β-mercaptoethanol, and 5% glycerol for 16 hr at 4°C. Reconstituted PA28αβ complexes were then purified by gel filtration on a HiPrep Sephacryl-S200 HR column (GE Healthcare, Piscataway, NJ) (Figure S1D) and were free of any exo- or endoproteolytic activity. PA28αβ-20S immunoproteasomes were reconstituted by preincubating 20S particles with an 8-fold molar excess of PA28αβ at 37°C for 30 min in 20 mM HEPES, pH 7.6, and 2 mM NaCl and were used immediately for degradation experiments. Native PAGE showed almost complete conversion of 20S particles into doubly capped (PA28αβ-20S-PA28αβ) 20S immunoproteasomes that were stable throughout the entire degradation period (Figure S1A). For analysis of peptide products, casein (470 μM) and denatured IGF-1 (900 μM) were incubated with 20S (20 nM IGF-1 and 50 nM casein), PA28αβ-20S (20 nM IGF-1 and 50 nM casein), and 26S immunoproteasomes (35 nM for both substrates) for 6 hr at 37°C in 20 mM HEPES, pH 7.6, 1.5 mM ATP, 3 mM $MgCl_2$, and 2 mM NaCl. To assay peptides generated during protein degradation, we measured the appearance of new amino groups using fluorescamine. At the end of the incubation, peptide products were separated from undegraded protein by ultrafiltration through a membrane with a 5 kDa cutoff, and these samples were used for HP-SEC and MS/MS. Consumption of substrates at the end of the incubation never exceeded 10% (Figure S2). FITC-casein (10 μM) was degraded by 20S, PA28αβ-20S, and 26S immunoproteasomes (40 nM) for 6 hr at 37°C in 20 mM HEPES, pH 7.6, 1.5 mM ATP, 3 mM $MgCl_2$, and 2 mM NaCl. At the end of the incubation, undigested FITC-casein was precipitated with 2% perchloric acid, and fluorescence in the supernatant was measured (excitation, 490 nm; emission, 525 nm). RP-HPLC analysis of peptides generated by different immunoproteasome species was performed using methods described elsewhere (Cascio et al., 2002). For HP-SEC, equal amounts of peptides generated during degradation of casein and IGF-1 were lyophilized, resuspended in 0.1 M HEPES, pH 6.8, and separated on a polyhydroxyethyl aspartamide column (0.46 × 20 cm; PolyLC, Columbia, MD). The mobile phase consisted of 0.2 M Na_2SO_4 and 25% acetonitrile, pH 3.0, at a flow rate of 0.125 ml/min. For each analysis, 20 μl of peptide solution was added to 10 μl of fluorescamine (0.3 mg/ml in acetone). The reaction was terminated after 30 s with 30 μl of H_2O, and the sample was immediately injected onto the HPLC column. The fluorescence of eluted material was monitored continuously, and a blank run (corresponding to time 0) was always subtracted. To determine the apparent molecular mass of peptides eluted, the column was calibrated with 18 standard amino acids and peptides in the 200 to 3,500 Da range that had been derivatized with fluorescamine in the same manner as proteasomal degradation products. Prior control studies showed that the retention times of these fluorescamine-derivatized products are highly reproducible and linearly dependent on the logarithm of their molecular weights (Figure S2) and that recovery of amino acids and peptides of different lengths is quantitative. Note that amino acids and peptides eluted from the column are bound to fluorescamine, whose molecular weight must be subtracted to calculate the actual mass of proteasomal products. Mean and median sizes of peptides generated by immunoproteasomes were calculated from the distributions of products obtained by HP-SEC, assuming an average molecular weight of 110 Da for each residue. Proteasome peptidase activities were measured using specific fluorogenic substrates in 20 mM Tris-HCl, pH 7.5, 1 mM ATP, 2 mM $MgCl_2$, and 0.2% (w/v) BSA. The fluorescence of released 7-amino-4-methylcoumarin (excitation, 380 nm; emission, 460 nm) was monitored continuously at 37°C. Assays were calibrated using standard solutions of the free fluorophore, and the reaction velocities were calculated from the slopes of the initial linear portions of the curves.

Tandem Mass Spectrometry of Proteasomal Products

Peptides generated by degradation of similar amounts of IGF-1 by immunoproteasomes and casein in two independent experiments were analyzed by liquid chromatography-MS/MS. Peptides were captured on a C18 column stage tip. The cleaned peptides were separated on a nano-HPLC system (EASY-nLC; Proxeon/Thermo Fisher Scientific, West Palm Beach, FL) using

a 5% to 40% linear gradient of acetonitrile on a 15-cm microcolumn (prepared in house; 75-μm inner diameter, filled with 3-μm C18 reverse phase beads, ReproSil column; Dr. Maisch, Ammerbuch-Entringen, Germany) and directly sprayed into the mass spectrometer (LTQ Orbitrap or Q Exactive; Thermo Fisher Scientific) using a Proxeon ion source. Data were analyzed using version 1.3.0.5 of the MaxQuant software package (Cox and Mann, 2008). Briefly, the software uses MS/MS spectra for the identification of peptides, and quantification of peptides is derived from MS/MS spectra. The software integrates the intensities over the entire range of elution, thus allowing highly accurate quantification of peptides. The false discovery rate was set to 1% of peptide levels.

Statistical Analyses

To compare average measures of amino group generation, protein degradation, and peptide hydrophilicity, we adopted a Mann-Whitney U test. Error bars represent SEM.

SUPPLEMENTAL INFORMATION

Supplemental Information includes Supplemental Experimental Procedures, two figures, and three tables and can be found with this article online at http://dx.doi.org/10.1016/j.chembiol.2014.02.006.

ACKNOWLEDGMENTS

We thank Marion Schmidt and Ernst Jarosch for critical reading of the manuscript, and we are grateful to Patrick Moore for assistance in preparation of the manuscript. This research was supported by the Italian Ministry of Instruction, University and Research (MIUR) (PRIN 2008 to P.C.).

Received: July 25, 2013
Revised: December 20, 2013
Accepted: February 3, 2014
Published: March 13, 2014

REFERENCES

Ahn, K., Erlander, M., Leturcq, D., Peterson, P.A., Früh, K., and Yang, Y. (1996). In vivo characterization of the proteasome regulator PA28. J. Biol. Chem. *271*, 18237–18242.

Bantscheff, M., Schirle, M., Sweetman, G., Rick, J., and Kuster, B. (2007). Quantitative mass spectrometry in proteomics: a critical review. Anal. Bioanal. Chem. *389*, 1017–1031.

Benaroudj, N., Zwickl, P., Seemüller, E., Baumeister, W., and Goldberg, A.L. (2003). ATP hydrolysis by the proteasome regulatory complex PAN serves multiple functions in protein degradation. Mol. Cell *11*, 69–78.

Berko, D., Tabachnick-Cherny, S., Shental-Bechor, D., Cascio, P., Mioletti, S., Levy, Y., Admon, A., Ziv, T., Tirosh, B., Goldberg, A.L., and Navon, A. (2012). The direction of protein entry into the proteasome determines the variety of products and depends on the force needed to unfold its two termini. Mol. Cell *48*, 601–611.

Cascio, P., Hilton, C., Kisselev, A.F., Rock, K.L., and Goldberg, A.L. (2001). 26S proteasomes and immunoproteasomes produce mainly N-extended versions of an antigenic peptide. EMBO J. *20*, 2357–2366.

Cascio, P., Call, M., Petre, B.M., Walz, T., and Goldberg, A.L. (2002). Properties of the hybrid form of the 26S proteasome containing both 19S and PA28 complexes. EMBO J. *21*, 2636–2645.

Coux, O., Tanaka, K., and Goldberg, A.L. (1996). Structure and functions of the 20S and 26S proteasomes. Annu. Rev. Biochem. *65*, 801–847.

Cox, J., and Mann, M. (2008). MaxQuant enables high peptide identification rates, individualized p.p.b.-range mass accuracies and proteome-wide protein quantification. Nat. Biotechnol. *26*, 1367–1372.

de Graaf, N., van Helden, M.J., Textoris-Taube, K., Chiba, T., Topham, D.J., Kloetzel, P.M., Zaiss, D.M., and Sijts, A.J. (2011). PA28 and the proteasome immunosubunits play a central and independent role in the production of MHC class I-binding peptides in vivo. Eur. J. Immunol. *41*, 926–935.

Dick, T.P., Ruppert, T., Groettrup, M., Kloetzel, P.M., Kuehn, L., Koszinowski, U.H., Stevanović, S., Schild, H., and Rammensee, H.G. (1996). Coordinated dual cleavages induced by the proteasome regulator PA28 lead to dominant MHC ligands. Cell *86*, 253–262.

Dolenc, I., Seemüller, E., and Baumeister, W. (1998). Decelerated degradation of short peptides by the 20S proteasome. FEBS Lett. *434*, 357–361.

Dubiel, W., Pratt, G., Ferrell, K., and Rechsteiner, M. (1992). Purification of an 11S regulator of the multicatalytic protease. J. Biol. Chem. *267*, 22369–22377.

Groll, M., Bajorek, M., Köhler, A., Moroder, L., Rubin, D.M., Huber, R., Glickman, M.H., and Finley, D. (2000). A gated channel into the proteasome core particle. Nat. Struct. Biol. *7*, 1062–1067.

Harris, J.L., Alper, P.B., Li, J., Rechsteiner, M., and Backes, B.J. (2001). Substrate specificity of the human proteasome. Chem. Biol. *8*, 1131–1141.

Hendil, K.B., Khan, S., and Tanaka, K. (1998). Simultaneous binding of PA28 and PA700 activators to 20S proteasomes. Biochem. J. *332*, 749–754.

Kincaid, E.Z., Che, J.W., York, I., Escobar, H., Reyes-Vargas, E., Delgado, J.C., Welsh, R.M., Karow, M.L., Murphy, A.J., Valenzuela, D.M., et al. (2012). Mice completely lacking immunoproteasomes show major changes in antigen presentation. Nat. Immunol. *13*, 129–135.

Kisselev, A.F., Akopian, T.N., Woo, K.M., and Goldberg, A.L. (1999). The sizes of peptides generated from protein by mammalian 26 and 20S proteasomes. Implications for understanding the degradative mechanism and antigen presentation. J. Biol. Chem. *274*, 3363–3371.

Kloetzel, P.M. (2001). Antigen processing by the proteasome. Nat. Rev. Mol. Cell Biol. *2*, 179–187.

Knowlton, J.R., Johnston, S.C., Whitby, F.G., Realini, C., Zhang, Z., Rechsteiner, M., and Hill, C.P. (1997). Structure of the proteasome activator REGα (PA28α). Nature *390*, 639–643.

Köhler, A., Cascio, P., Leggett, D.S., Woo, K.M., Goldberg, A.L., and Finley, D. (2001). The axial channel of the proteasome core particle is gated by the Rpt2 ATPase and controls both substrate entry and product release. Mol. Cell *7*, 1143–1152.

Li, J., Gao, X., Joss, L., and Rechsteiner, M. (2000). The proteasome activator 11S REG or PA28: chimeras implicate carboxyl-terminal sequences in oligomerization and proteasome binding but not in the activation of specific proteasome catalytic subunits. J. Mol. Biol. *299*, 641–654.

Li, J., Gao, X., Ortega, J., Nazif, T., Joss, L., Bogyo, M., Steven, A.C., and Rechsteiner, M. (2001). Lysine 188 substitutions convert the pattern of proteasome activation by REGγ to that of REGs α and β. EMBO J. *20*, 3359–3369.

Li, J., Powell, S.R., and Wang, X. (2011). Enhancement of proteasome function by PA28α: overexpression protects against oxidative stress. FASEB J. *25*, 883–893.

Ma, C.P., Slaughter, C.A., and DeMartino, G.N. (1992). Identification, purification, and characterization of a protein activator (PA28) of the 20S proteasome (macropain). J. Biol. Chem. *267*, 10515–10523.

Mishto, M., Luciani, F., Holzhütter, H.G., Bellavista, E., Santoro, A., Textoris-Taube, K., Franceschi, C., Kloetzel, P.M., and Zaikin, A. (2008). Modeling the in vitro 20S proteasome activity: the effect of PA28-αβ and of the sequence and length of polypeptides on the degradation kinetics. J. Mol. Biol. *377*, 1607–1617.

Murata, S., Udono, H., Tanahashi, N., Hamada, N., Watanabe, K., Adachi, K., Yamano, T., Yui, K., Kobayashi, N., Kasahara, M., et al. (2001). Immunoproteasome assembly and antigen presentation in mice lacking both PA28α and PA28β. EMBO J. *20*, 5898–5907.

Old, W.M., Meyer-Arendt, K., Aveline-Wolf, L., Pierce, K.G., Mendoza, A., Sevinsky, J.R., Resing, K.A., and Ahn, N.G. (2005). Comparison of label-free methods for quantifying human proteins by shotgun proteomics. Mol. Cell. Proteomics *4*, 1487–1502.

Orlowski, M., and Wilk, S. (2003). Ubiquitin-independent proteolytic functions of the proteasome. Arch. Biochem. Biophys. *415*, 1–5.

Osmulski, P.A., and Gaczynska, M. (2000). Atomic force microscopy reveals two conformations of the 20S proteasome from fission yeast. J. Biol. Chem. *275*, 13171–13174.

Osmulski, P.A., and Gaczynska, M. (2002). Nanoenzymology of the 20S proteasome: proteasomal actions are controlled by the allosteric transition. Biochemistry *41*, 7047–7053.

Osmulski, P.A., Hochstrasser, M., and Gaczynska, M. (2009). A tetrahedral transition state at the active sites of the 20S proteasome is coupled to opening of the α-ring channel. Structure *17*, 1137–1147.

Pamer, E., and Cresswell, P. (1998). Mechanisms of MHC class I-restricted antigen processing. Annu. Rev. Immunol. *16*, 323–358.

Pickering, A.M., Koop, A.L., Teoh, C.Y., Ermak, G., Grune, T., and Davies, K.J. (2010). The immunoproteasome, the 20S proteasome and the PA28αβ proteasome regulator are oxidative-stress-adaptive proteolytic complexes. Biochem. J. *432*, 585–594.

Qian, S.B., Princiotta, M.F., Bennink, J.R., and Yewdell, J.W. (2006). Characterization of rapidly degraded polypeptides in mammalian cells reveals a novel layer of nascent protein quality control. J. Biol. Chem. *281*, 392–400.

Rabl, J., Smith, D.M., Yu, Y., Chang, S.C., Goldberg, A.L., and Cheng, Y. (2008). Mechanism of gate opening in the 20S proteasome by the proteasomal ATPases. Mol. Cell *30*, 360–368.

Rechsteiner, M., Realini, C., and Ustrell, V. (2000). The proteasome activator 11S REG (PA28) and class I antigen presentation. Biochem. J. *345*, 1–15.

Rock, K.L., and Goldberg, A.L. (1999). Degradation of cell proteins and the generation of MHC class I-presented peptides. Annu. Rev. Immunol. *17*, 739–779.

Ruschak, A.M., and Kay, L.E. (2012). Proteasome allostery as a population shift between interchanging conformers. Proc. Natl. Acad. Sci. USA *109*, E3454–E3462.

Saric, T., Graef, C.I., and Goldberg, A.L. (2004). Pathway for degradation of peptides generated by proteasomes: a key role for thimet oligopeptidase and other metallopeptidases. J. Biol. Chem. *279*, 46723–46732.

Shabek, N., and Ciechanover, A. (2010). Degradation of ubiquitin: the fate of the cellular reaper. Cell Cycle *9*, 523–530.

Sijts, A., Sun, Y., Janek, K., Kral, S., Paschen, A., Schadendorf, D., and Kloetzel, P.M. (2002). The role of the proteasome activator PA28 in MHC class I antigen processing. Mol. Immunol. *39*, 165–169.

Song, X., von Kampen, J., Slaughter, C.A., and DeMartino, G.N. (1997). Relative functions of the α and β subunits of the proteasome activator, PA28. J. Biol. Chem. *272*, 27994–28000.

Stadtmueller, B.M., and Hill, C.P. (2011). Proteasome activators. Mol. Cell *41*, 8–19.

Stohwasser, R., Salzmann, U., Giesebrecht, J., Kloetzel, P.M., and Holzhütter, H.G. (2000). Kinetic evidences for facilitation of peptide channelling by the proteasome activator PA28. Eur. J. Biochem. *267*, 6221–6230.

Sugiyama, M., Sahashi, H., Kurimoto, E., Takata, S., Yagi, H., Kanai, K., Sakata, E., Minami, Y., Tanaka, K., and Kato, K. (2013). Spatial arrangement and functional role of α subunits of proteasome activator PA28 in hetero-oligomeric form. Biochem. Biophys. Res. Commun. *432*, 141–145.

Tanahashi, N., Yokota, K., Ahn, J.Y., Chung, C.H., Fujiwara, T., Takahashi, E., DeMartino, G.N., Slaughter, C.A., Toyonaga, T., Yamamura, K., et al. (1997). Molecular properties of the proteasome activator PA28 family proteins and γ-interferon regulation. Genes Cells *2*, 195–211.

Voges, D., Zwickl, P., and Baumeister, W. (1999). The 26S proteasome: a molecular machine designed for controlled proteolysis. Annu. Rev. Biochem. *68*, 1015–1068.

Whitby, F.G., Masters, E.I., Kramer, L., Knowlton, J.R., Yao, Y., Wang, C.C., and Hill, C.P. (2000). Structural basis for the activation of 20S proteasomes by 11S regulators. Nature *408*, 115–120.

Yamano, T., Sugahara, H., Mizukami, S., Murata, S., Chiba, T., Tanaka, K., Yui, K., and Udono, H. (2008). Allele-selective effect of PA28 in MHC class I antigen processing. J. Immunol. *181*, 1655–1664.

Yao, T., and Cohen, R.E. (2002). A cryptic protease couples deubiquitination and degradation by the proteasome. Nature *419*, 403–407.

Yewdell, J.W. (2001). Not such a dismal science: the economics of protein synthesis, folding, degradation and antigen processing. Trends Cell Biol. *11*, 294–297.

Yuksek, K., Chen, W.L., Chien, D., and Ou, J.H. (2009). Ubiquitin-independent degradation of hepatitis C virus F protein. J. Virol. *83*, 612–621.

Zhang, Z., Realini, C., Clawson, A., Endicott, S., and Rechsteiner, M. (1998). Proteasome activation by REG molecules lacking homolog-specific inserts. J. Biol. Chem. *273*, 9501–9509.

